

Supplementary Materials for

Applicability of physics-based and machine-learning-based algorithms of geostationary satellite in retrieving the diurnal cycle of cloud base height

Mengyuan Wang¹, Min Min^{1*}, Jun Li², Han Lin³, Yongen Liang¹,
Binlong Chen², Zhigang Yao⁴, Na Xu², Miao Zhang²

1 School of Atmospheric Sciences, Southern Marine Science and Engineering Guangdong Laboratory (Zhuhai), and Guangdong Province Key Laboratory for Climate Change and Natural Disaster Studies, Zhuhai 519082, China

2 Key Laboratory of Radiometric Calibration and Validation for Environmental Satellites and Innovation Center for FengYun Meteorological Satellite (FYSIC), National Satellite Meteorological Center (National Center for Space Weather), China Meteorological Administration, Beijing 100081, China

3 Key Laboratory of Spatial Data Mining and Information Sharing of Ministry of Education, National and Local Joint Engineering Research Center of Satellite Geospatial Information Technology, Fuzhou University, Fuzhou 350108, China

4 Beijing Institute of Applied Meteorology, Beijing 100029, China

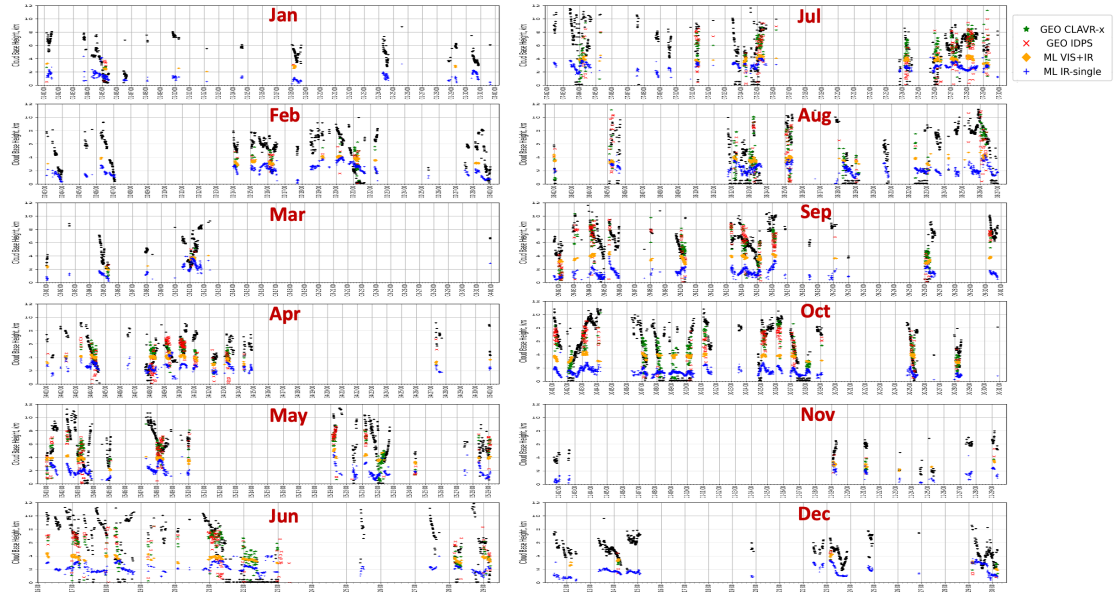


Fig. S1. Same as Figure 6, monthly comparisons of CBHs from four GEO satellite algorithms with the CBH sample results from Cloud radar at Beijing Nanjiao station (black solid circle).

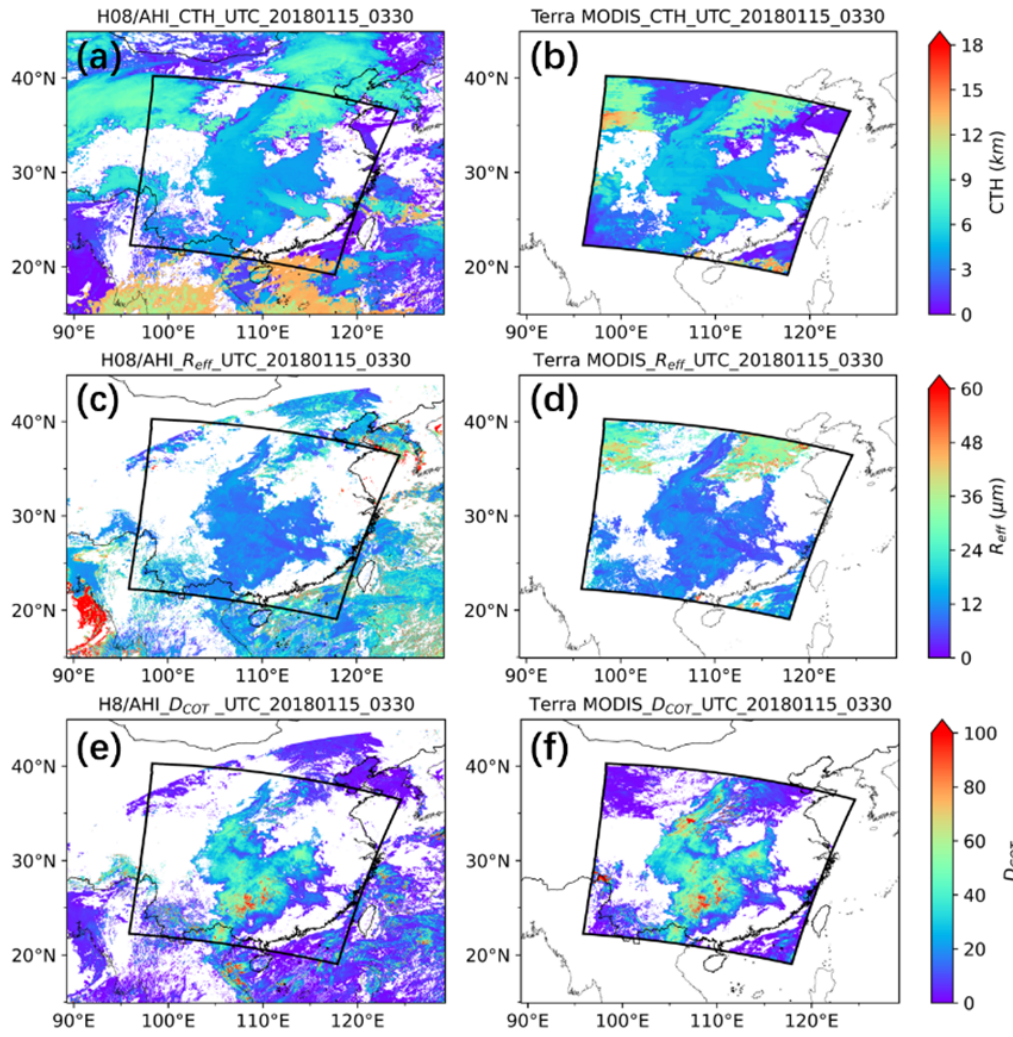


Fig. S2. Comparison of CTH (top row panel), D_{COT} (middle row panel), and R_{eff} (bottom row panel) from Himawari-8 and operational Terra/MODIS(MYD06) at 03:30 UTC on January 15, 2018.

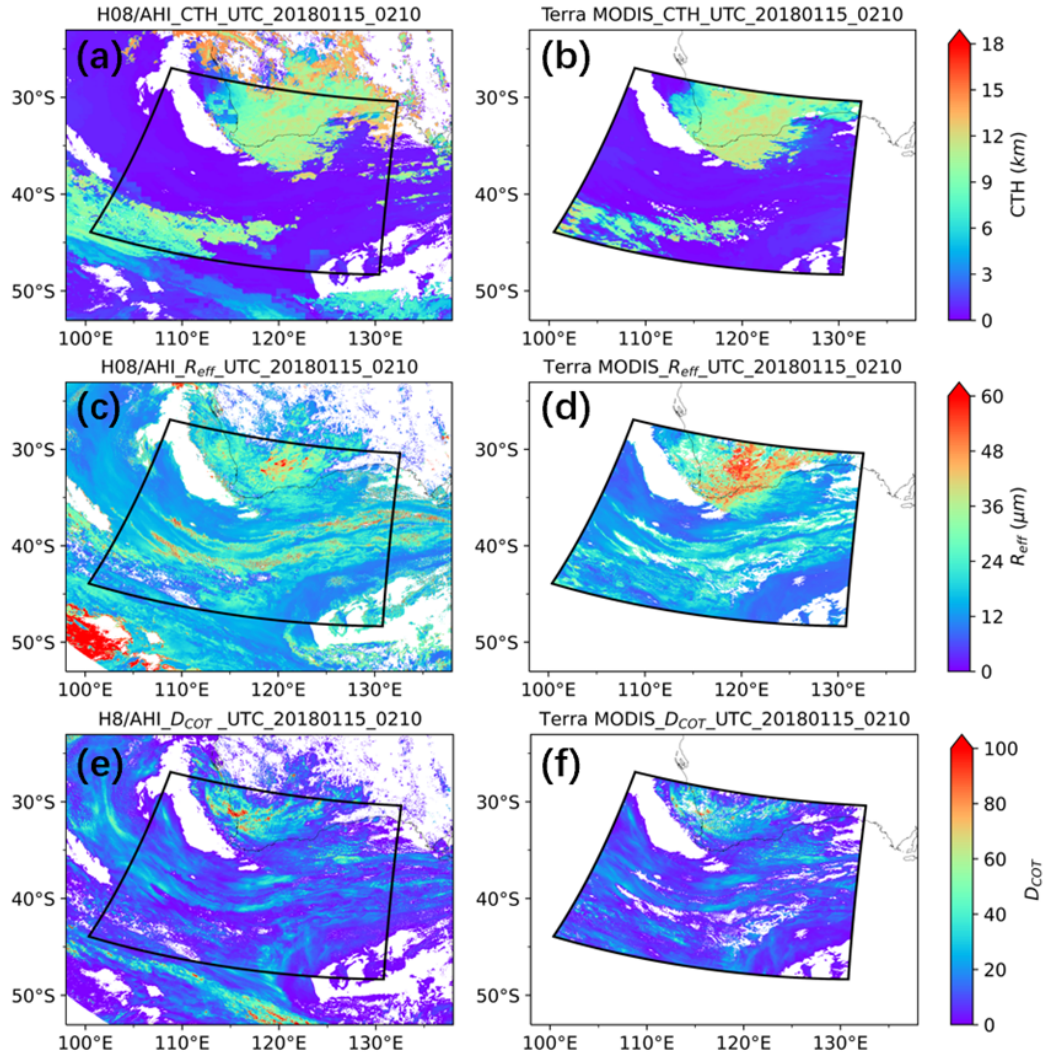


Fig. S3. The same as Fig. A1, but for the case at 02:10 UTC on January 15, 2018.

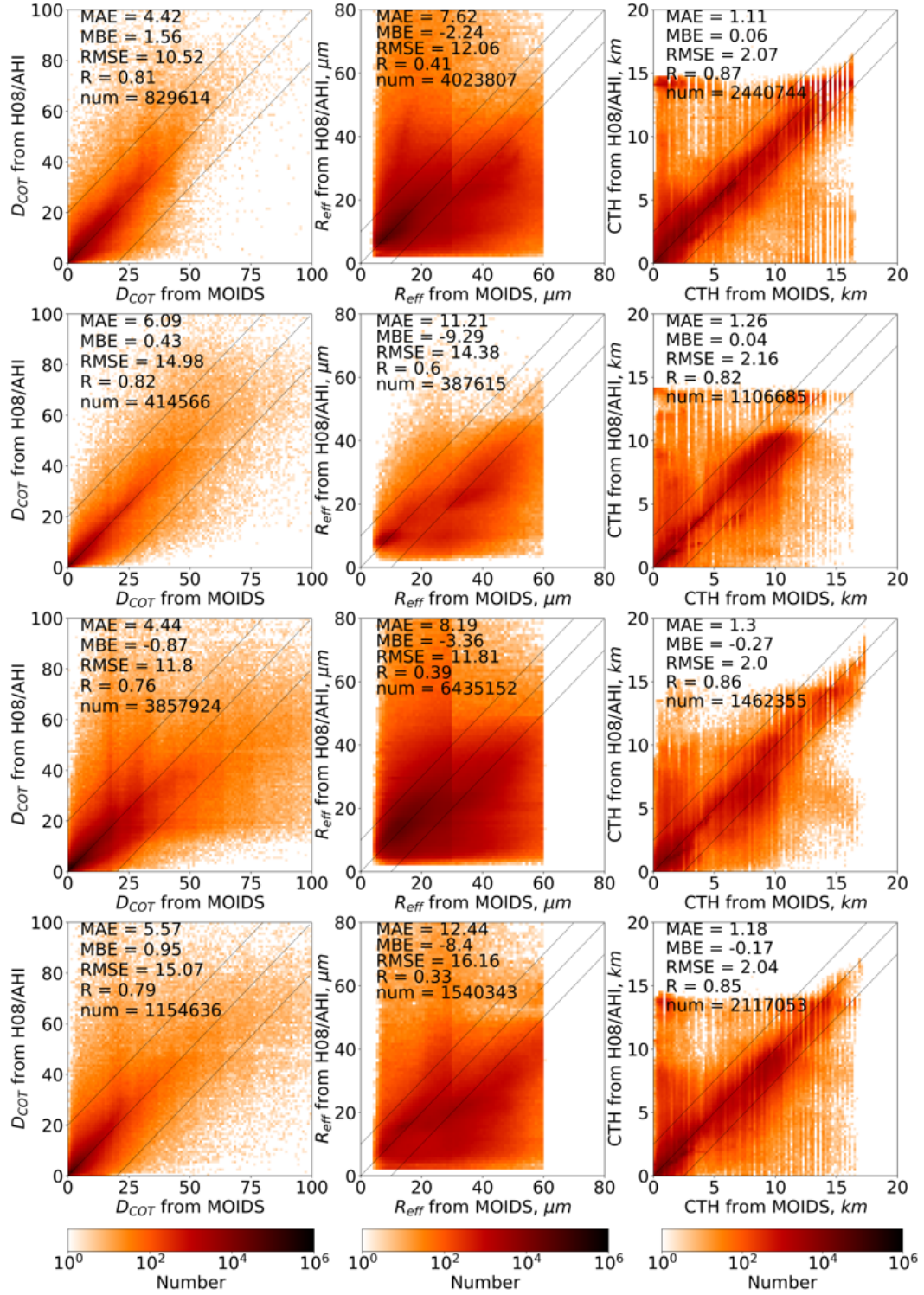


Fig. S4. Comparisons of D_{cor} (left column panel), R_{eff} (middle column panel), CTH (right column panel) between H8/AHI and MODIS in January (first row panel), April (second row panel), July (third row panel) and October (fourth row panel) of 2018.

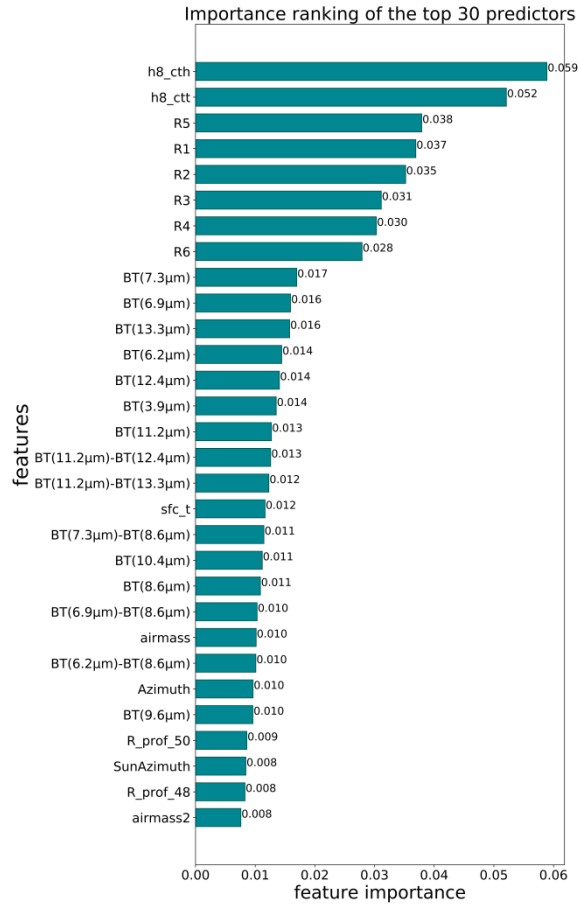


Fig. S5. Importance ranking of the top 30 predictors in the VIS+IR RF model. (airmass = $\text{AirMass}(1/\cos(\text{VZA}))$, airmass2= $\text{AirMass}(1/\cos(\text{SZA}))$, $R_i = \text{airmass2} \times \text{BTD}_i \times 0.01$). sfc_t means the temperature at the surface and R_prof means the relative humidity at the surface.

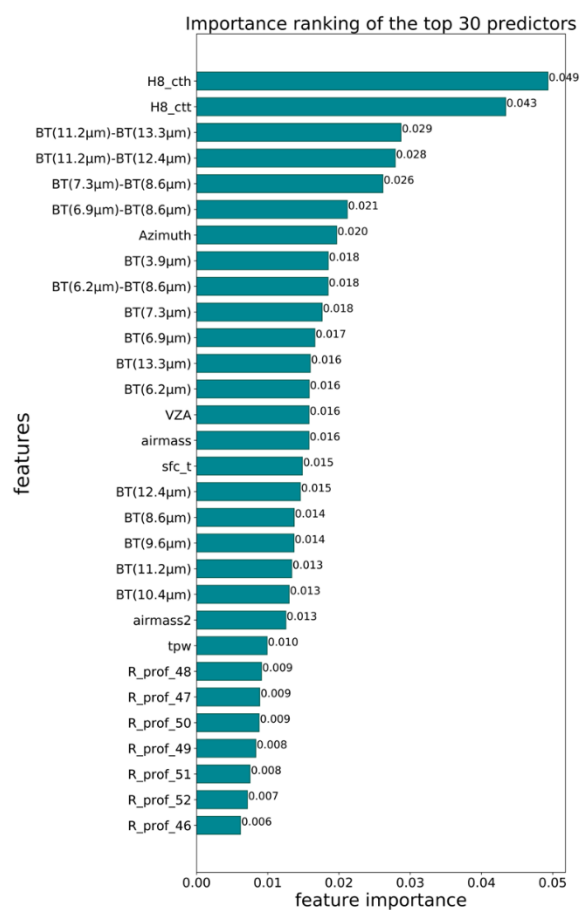


Fig. S6. The same as Fig. S5, but for the IR-single RF model.

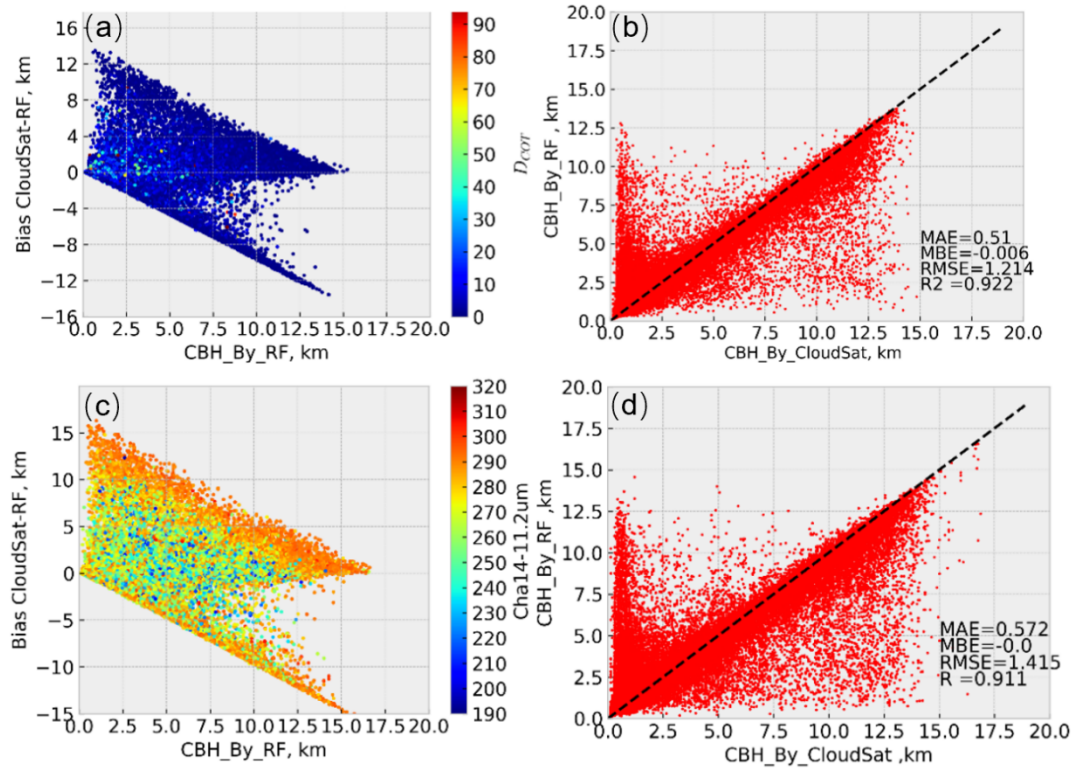


Fig. S7. Scatterplots of the CBHs retrieved by the IR-single model algorithm (a) before and (b) after optimization compared with the CBHs from the joint CALIPSO/CloudSat product. The subfigures (c) and (d) are the same as subfigures (a) and (b), but for the IR brightness temperature values.

Table S1. Range of filtered D_{COT} values and the calculated correlation statistics MAE, MBE, RMSE, R and the number of matched points filtered out.

$<D_{\text{COT}}$	MAE	MBE	RMSE	R	drop number
0.3	0.705	−0.018	1.651	0.895	6
0.4	0.705	−0.018	1.651	0.895	68
0.5	0.703	−0.017	1.648	0.895	344
0.6	0.695	−0.017	1.631	0.895	969
0.7	0.68	−0.018	1.599	0.896	2149
0.8	0.653	−0.016	1.542	0.899	3895
0.9	0.626	−0.012	1.485	0.903	5430
1.0	0.603	−0.01	1.431	0.907	6810
1.1	0.585	−0.011	1.39	0.91	8140
1.2	0.568	−0.009	1.352	0.913	9291
1.3	0.551	−0.008	1.312	0.916	10476
1.4	0.535	−0.009	1.273	0.919	11586
1.5	0.523	−0.008	1.245	0.92	12607
1.6	0.51	−0.006	1.214	0.922	13751
1.7	0.499	−0.008	1.186	0.923	14833
1.8	0.49	−0.009	1.162	0.925	15699
1.9	0.48	−0.01	1.14	0.926	16574
2.0	0.469	−0.009	1.112	0.928	17469
2.1	0.459	−0.01	1.083	0.93	18361
2.2	0.451	−0.011	1.066	0.931	19218
2.3	0.443	−0.012	1.046	0.932	20080
2.4	0.436	−0.011	1.029	0.933	20878
2.5	0.431	−0.011	1.015	0.933	21630
2.6	0.425	−0.012	0.999	0.934	22453
2.7	0.418	−0.012	0.982	0.935	23282
2.8	0.414	−0.012	0.971	0.936	23980
2.9	0.409	−0.011	0.96	0.936	24685
3.0	0.405	−0.012	0.95	0.936	25360
3.1	0.402	−0.012	0.944	0.936	26042
3.2	0.398	−0.013	0.934	0.936	26778
3.3	0.393	−0.014	0.923	0.936	27492
3.4	0.389	−0.014	0.913	0.937	28127
3.5	0.384	−0.016	0.9	0.937	28793
3.6	0.379	−0.016	0.889	0.938	29465
3.7	0.376	−0.016	0.882	0.938	30128
3.8	0.372	−0.017	0.87	0.938	30772
3.9	0.368	−0.017	0.862	0.939	31388

Table S2. Range of filtered IR channel 14 values and the calculated correlation statistics MAE, MBE, RMSE, R and the number of matched points filtered out.

Cha14	MAE	MBE	RMSE	R	drop numbers
270	0.538	−0.005	1.293	0.924	35490
271	0.541	−0.006	1.301	0.923	33922
272	0.541	−0.006	1.307	0.922	32187
273	0.544	−0.006	1.315	0.921	30483
274	0.544	−0.006	1.32	0.921	28723
275	0.545	−0.004	1.327	0.92	26949
276	0.547	−0.004	1.336	0.919	25169
277	0.55	−0.003	1.35	0.917	23408
278	0.556	−0.004	1.366	0.916	21769
279	0.562	−0.002	1.384	0.914	20307
280	0.567	−0.002	1.399	0.913	18676
281	0.572	0	1.415	0.911	16917
282	0.579	0	1.435	0.909	15228
283	0.587	0.001	1.455	0.907	13748
284	0.595	0.002	1.478	0.905	12233
285	0.605	0.001	1.503	0.903	10720
286	0.617	0.001	1.531	0.901	9305
287	0.632	0	1.568	0.897	8083
288	0.65	0.002	1.612	0.893	6839
289	0.667	0.001	1.654	0.89	5708
290	0.686	0	1.698	0.886	4606
291	0.703	0.001	1.737	0.884	3552
292	0.725	−0.001	1.785	0.88	2675
293	0.747	−0.004	1.838	0.875	1874
294	0.762	−0.006	1.875	0.872	1202
295	0.772	−0.007	1.897	0.87	704
296	0.78	−0.008	1.918	0.868	370
297	0.782	−0.007	1.923	0.868	262
298	0.782	−0.007	1.923	0.868	217
299	0.782	−0.007	1.923	0.868	183